P3.29 KINEMATIC AND MICROPHYSICAL STRUCTURES OF MULTI-CELLULAR STORM DEVELOPING OVER THE ZOSHIGAYA AREA OF TOKYO, JAPAN

D.-S. Kim[1], M. Maki[1], S. Shimizu[1], T. Maesaka[1], K. Iwanami[1] and D.-I. Lee[2]

[1]National Research Institute for Earth Science and Disaster Prevention, Tsukuba, Japan
[2]Department of Environmental Atmospheric Sciences, Pukyong National University, Busan, Korea

1. INTRODUCTION

Multi-cellular storms often develop over the southern Kanto Plain of Japan, generating heavy rainfall that may cause urban flooding and landslides, especially when the storm cells are mature and slow moving. A multi-cellular storm is defined as a storm comprising several precipitating convective cells that may persist for several hours due to the periodic appearance of new cells. The individual embedded cells are generated from the quasi-steady updraft cell located over the leading edge of the density current (Lin et al. 1998) and are normally short-lived, lasting about 15–30 min (Browning et al. 1976; Hobbs and Locatelli 1978; Warner et al. 1980; Takeda and Seko 1986). Although most cells are short-lived, some may persist for several hours or more (herein referred to as long-lasting convective cells).

We present here a case study of a multi-cellular storm observed in the Zoshigaya area of Tokyo, Japan on 5 August 2008. This storm produced localized, severe rainfall, and resulted in five sewer workers being swept away by a flash flood (Kato and Maki 2009; Hirano and Maki 2010). Unique to this study are the dual-polarization measurements made using X-band wavelength radar. The aim of this study is to investigate the precipitation core and kinematic structure of the individual precipitation cells within this storm by analyzing measurements from two X-band polarization radars.

2. DATA

Two X-band dual-polarization radars (at Ebina and Kisarazu), operated by the National Research Institute for Earth Science and Disaster Prevention (NIED) of Japan, were used to observe a storm over Tokyo, Japan (Fig. 1).

The Ebina and Kisarazu radars simultaneously transmit and receive horizontally and vertically polarized signals at frequencies of 9.375 GHz (Ebina) and 9.709 GHz (Kisarazu). The polarimetric variables radar reflectivity factor at horizontal polarization (Z_H), differential reflectivity (Z_{DR}) and the specific differential phase shift (K_{DP}) obtained from Ebina were used primarily to analyze the structure of the storm. Velocity data obtained from both radar stations were used to analyze the kinematic structure of the storm. The Z_H and Z_{DR} biases were estimated to be 5.6 dBZ and –1.44 dB, respectively, according to the method of Gorgucci et al. (1999). The observed Z_H and Z_{DR} were also corrected for rain attenuation using the attenuation correction algorithm proposed by

Kim et al. (2008, 2010), which considers variability in the optimum coefficient α ($A_H = \alpha K_{DP}$) along the radar slant-range.

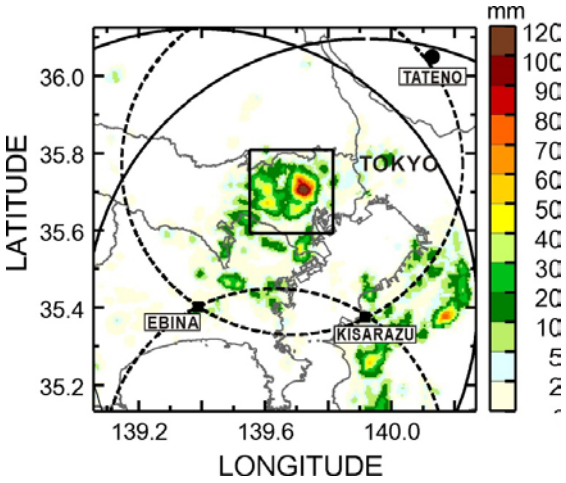

Fig. 1. Map showing the observation domain and data collection methods. The Ebina and Kisarazu radars (■) each covered a radius of 80 km. Dual-Doppler radar analysis was conducted within the gray area. Sounding data were obtained at ● Tateno ( ). Three-dimensional analysis of the precipitation core was conducted within the area shown by the box in the gray area.

The precipitation cells and cores were defined by their LWC estimated from K_{DP}, mainly in convective echo, as well as Z_H. A composite method was used to derive LWC from scattering simulations performed at a temperature of 15°C and with Andsager's drop shape (Maki et al. 2005), as follows:

$$LWC(Z_H; K_{DP}) = \begin{cases} 0.00393 Z_H^{0.55} \\ 0.991 K_{DP}^{0.713} \end{cases}$$

$$\begin{matrix} for \;\; K_{DP} \le 0.3 \;\; \deg km^{-1} \;\; or \;\; Z_H \le 35 dBZ \\ for \;\; K_{DP} > 0.3 \;\; \deg km^{-1} \end{matrix} \qquad (1)$$

When $K_{DP} > 0.3°$ km^{-1}, which is the estimated standard error of K_{DP}, the LWC–K_{DP} relationship can be used to calculate LWC. However, for $K_{DP} \le 0.3$ ° km^{-1} or $Z_H \le 35$ dB, the LWC–Z_H relationship is used because K_{DP} is noisy. Convective cells were defined as the region enclosing a single peak of LWC in a 3-dimentional distribution at all height up to echo top. However, two peaks of LWC at upper height (4 km) was merged while descending within 5 minute, it was regarded to one convective cell. We conducted a dual-Doppler analysis using the variation method proposed by Gao et al. (1999). Three components of wind were calculated in the Cartesian coordinate system within the gray area in Fig. 1a (the intersection angle is less than 30°).

3. RESULTS

Between 1100 and 1305 LST, multi-cellular storms over the study area were monitored and classified into 20 precipitation cells and two lifetime types: (1) short-lived cells (less than 30 minutes) and (2) long-lasting cells (more than 30 minutes). Long-lasting cell LC_1 (Table 1) was accompanied by heavy rainfall over the Zoshigaya area and its lifetime of 100 minutes is approximately 3–5 times longer than typically observed (20–30 minutes; see Byres and Braham 1949; Takeda and Imai 1976; Henry 1993).

The position of each precipitation cell (Fig. 2) was derived from the maximum LWC at any heights. Cells LC_1 and LC_2 moved northeastward at speeds of 1.1 and 2.2 m s^{-1}, respectively; they covered approximately 5 and 7 km during their lifetimes, but as these cells had horizontal extents of 5–8 km, they were in effect stationary. Most of the short-lived precipitation cells formed to the west of the long-lasting cell

LC_1, except those formed during the developmental stage of cell LC_1.

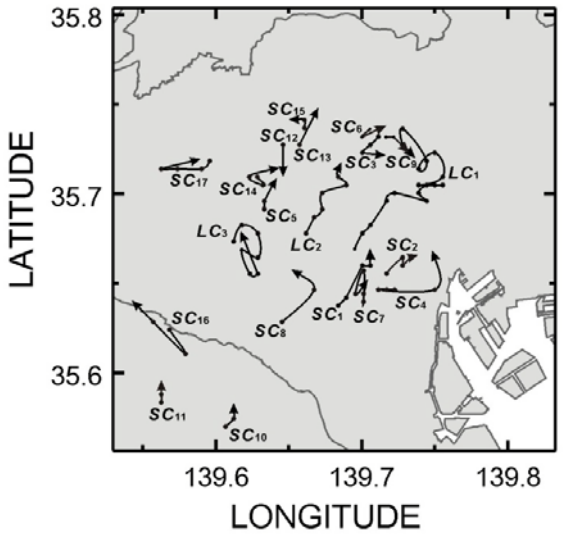

Fig. 2. Trajectories of the precipitation cells, defined by their maximum LWC values, within each precipitation cell in Table 1.

To investigate the temporal development of the core in short-lived precipitation cells, time series of the vertical profiles of the maximum LWC, updraft, and downdraft velocities were calculated for four short-lived cells (SC_4, SC_5, SC_7, and SC_8) (Fig. 3). Locations and ranges for each time period were selected to ensure that the strongest echoes at each height were included in the analysis. Maximum LWC values of 3.0–4.5 g m^{-3} were mostly observed below 6 km, and the precipitation cores gradually descended and reached the ground within 15–20 minutes. The rate of descent of these cores was 3.5–7.5 m s^{-1}. Strong updrafts (>4.5 m s^{-1}) were observed during the development stage of these short-lived cells. Cells SC_4, SC_5, SC_7, and SC_8 were created during the storm's

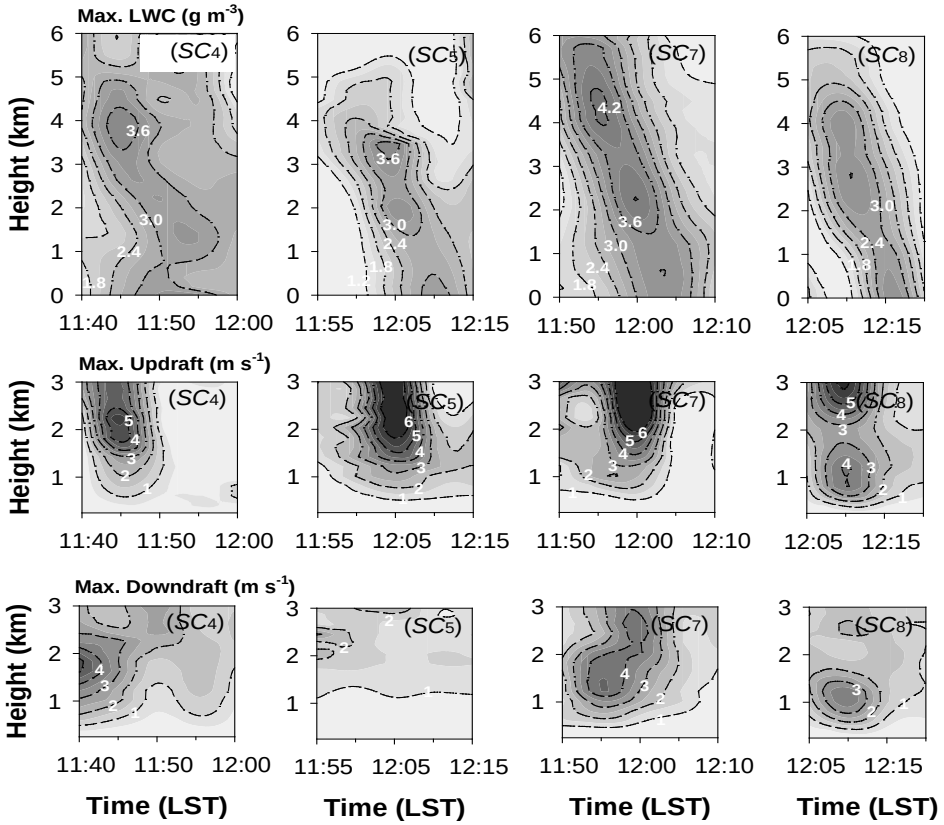

Fig. 3. Temporal change in vertical profiles of maximum LWC (top panel), maximum updraft (middle panel), and maximum downdraft (lower panel) for the short-lived cells SC_4, SC_5, SC_6, and SC_7.

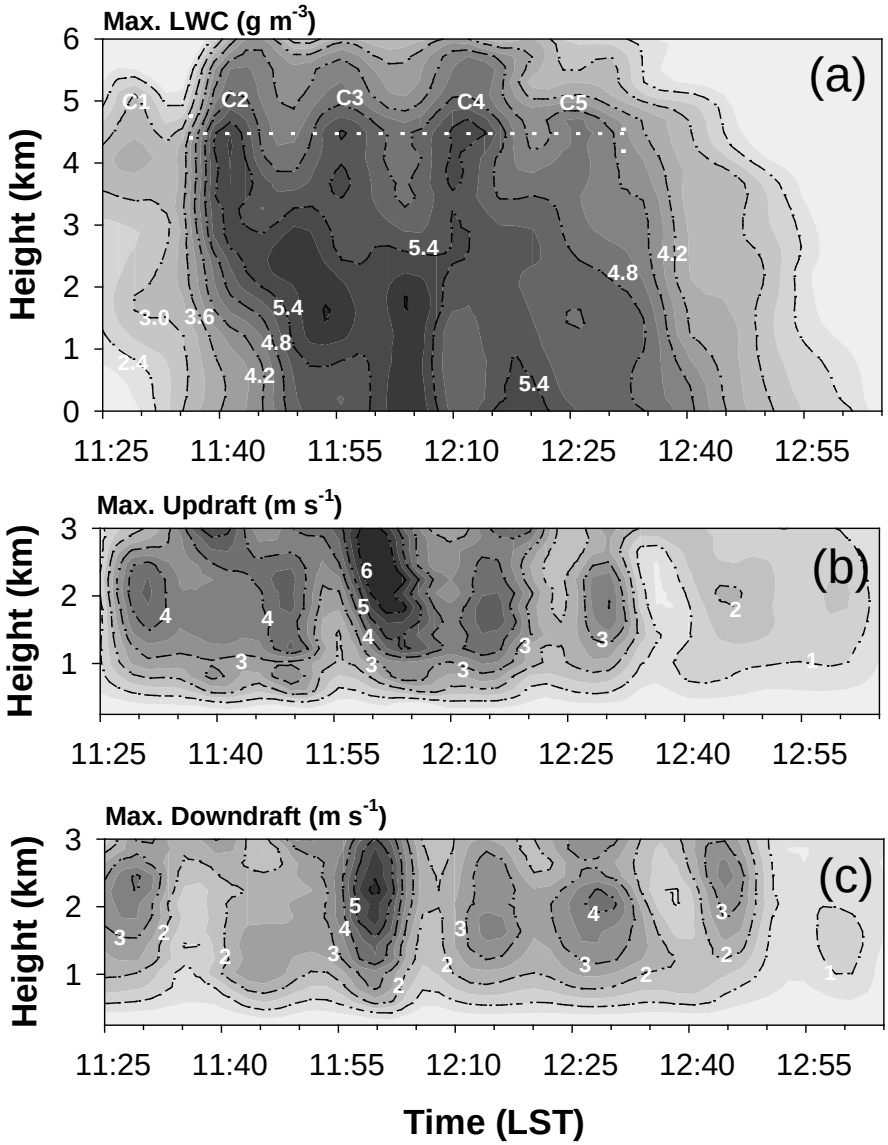

Fig. 4. As for Fig. 3, but for the long-lasting cell LC_1

early stage when a strong, low-level updraft (>5 m s^{-1}) occurred. The strong updrafts associated with the appearance of precipitation cores at upper levels showed a weakening during the dissipation stage. Downdrafts that first appeared during the developmental stage also weakened, but remained active, during the dissipation stage. Similar patterns of temporal evolution were observed (data not shown) in the other short-lived cells, and all of these short-lived cells had only one precipitation core that was generated by a low-level updraft and the cell dissipated by a downdraft.

On the other hand, at least five precipitation cores can be identified between 1125 and 1305 LST in the vertical profiles of maximum LWC, updraft, and downdraft in the long-lasting cell LC_1 (Fig. 4). These cores recurred every 15 minutes and most were associated with the strong updraft in the low-level atmosphere described above. At 1125 LST, the first precipitation core appears at around 4.5 km, growing slowly for the next 15 minutes but then developing rapidly due to a strong updraft at

1145 LST. During the mature stage (1145–1245 LST), four precipitation cores (C2–5) formed. Of these, three (C2–4) had a high LWC (>5.0 g m^{-3}), almost 1.5 times that of a typical short-lived cell. LWC was slightly lower (<5.0 g m^{-3}) in the last core (C5), although this is still relatively high compared with short-lived cells. These precipitation cores may have descended repeatedly, but it is difficult to distinguish each one clearly, especially between 1155 and 1210 LST, as the temporal resolution of the radar observations was too low. For example, one precipitation core descended toward the ground while a second was forming simultaneously in the upper levels. Generations of the five precipitation cores (C1–C5) in the upper levels during the developing and mature stages coincided with an increasing updraft at lower levels. During these stages (1125–1140 LST), an oscillation in intensity of downdraft as well as updraft were also observed at lower levels following the formation for precipitation cores, and the long-lasting cell LC_1 then dissipated slowly over about 20 minutes as the updraft weakened and the downdraft strengthened.

4. SUMMARY

A convective storm that produced 120 mm of rainfall during 2 hours and that caused flooding in the Zoshigaya area of Tokyo, Japan was analyzed using X-band polarimetric and dual-Doppler radar data. The storm comprised 20 precipitation cells, each with a precipitation core. The convective cells were classified as either a short-lived cell or long-lasting cell depending on the lifespan of the precipitation core. The first type, the ordinary (short-lived) precipitation cell, had an average lifetime of 16 minutes and 17 cells were classified as this type. These short-lived, ordinary cells are

Table 1. Number and lifetimes of precipitation cells that developed in the study area between 1100 and 1305 LST. Long-lasting type precipitation cells and short-lived type precipitation cells are indicated as *LC* and *SC*, respectively.

Type	Name of cell	Lifetime of precipitation cell		Rain (mm)	Max Area (km^2)
Long-lasting cell	LC_1	100 min	(1125-1305 LST)	100.62	48.75
	LC_2	40 min	(1145-1225 LST)	26.96	8.25
	LC_3	45 min	(1210-1255 LST)	37.19	24.75
Short-lived cell	SC_1	25 min	(1100-1125 LST)	17.01	9.50
	SC_2	25 min	(1125-1150 LST)	18.53	12.25
	SC_3	15 min	(1130-1145 LST)	13.02	12.34
	SC_4	20 min	(1140-1200 LST)	11.54	9.50
	SC_5	20 min	(1155-1215 LST)	11.37	14.00
	SC_6	10 min	(1155-1205 LST)	11.64	9.50
	SC_7	20 min	(1150-1210 LST)	15.17	18.25
	SC_8	15 min	(1205-1220 LST)	9.97	13.75
	SC_9	15 min	(1205-1220 LST)	12.77	8.00
	SC_{10}	10 min	(1205-1215 LST)	9.88	6.25
	SC_{11}	20 min	(1215-1235 LST)	16.93	10.25
	SC_{12}	5 min	(1220-1225 LST)	3.53	11.50
	SC_{13}	5 min	(1220-1225 LST)	3.52	9.00
	SC_{14}	15 min	(1225-1240 LST)	16.28	16.25
	SC_{15}	10 min	(1225-1235 LST)	5.87	7.25
	SC_{16}	20 min	(1235-1255 LST)	17.26	26.25
	SC_{17}	25 min	(1240-1305 LST)	18.94	30.25

Table 2. Maximum values of LWC, and maximum height of the LWC where it exceeds 3.0 g m^{-3}, for each precipitation cell. Also shown are the maximum updraft and downdraft velocities below a height of 3 km.

Name of cell	Max LWC (g m^{-3})	Max Height (km) of LWC ≥ 3.0 g m^{-3}	Max UW (m s^{-1}) of Height ≤ 3.0 km	Max DW (m s^{-1}) of Height ≤ 3.0 km
*LC*1	6.05	8.75	6.95	6.27
*LC*2	3.84	3.50	10.51	3.63
*LC*3	6.07	7.25	6.27	4.35
*SC*1	3.51	3.75	11.46	3.98
*SC*2	4.26	5.50	6.01	3.84
*SC*3	2.09	-	6.95	4.91
*SC*4	3.84	4.75	5.89	5.33
*SC*5	3.68	3.50	7.03	3.15
*SC*6	3.78	4.75	4.74	2.58
*SC*7	4.31	6.00	8.29	4.58
*SC*8	3.57	4.25	6.18	3.82
*SC*9	4.02	4.00	3.32	3.28
*SC*10	4.88	5.75	5.58	2.61
*SC*11	4.91	5.75	3.22	4.16
*SC*12	3.61	3.25	2.91	2.16
*SC*13	3.89	4.50	1.96	1.98
*SC*14	4.29	5.50	2.07	2.16
*SC*15	3.89	4.50	5.14	5.56
*SC*16	6.85	6.25	3.79	4.21
*SC*17	5.78	6.25	4.12	4.13

characterized by the descent of a single precipitation core. The second type of precipitation cell is the long-lasting type, and three cells were classified in this category with lifetimes of 100, 45, and 40 minutes. During the lifetime of the long-lasting cells, several precipitation cores were alternately produced and descended to the ground. The precipitation core in a short-lived cell appears with the development of a precipitation cell via updrafts associated with low-level convergence. The precipitation core falls to the ground within 5–25 minutes in the absence of a supporting updraft. In contrast, the replacement of precipitation cores in long-lasting cells is driven by periodic updrafts associated with a low-level southeasterly inflow that supplied warm, moist air to the precipitation cell. In this study we considered the structure and developmental mechanisms of precipitation cores with differing life cycles.

Table 2 summarizes the characteristics of the precipitation core (intensity and height) for each precipitation cell. The table also shows the maximum updraft and downdraft velocity at lower levels (below 3 km), as obtained from dual-Doppler analysis. The formation height of the precipitation cores in the long-lasting cell LC_1 was relatively high (~9 km), whereas the average height for short-lived cells was 4.1 km. The intensity and height of precipitation cores are proportionally related. The maximum updraft and downdraft velocities at lower levels (below 3 km) for the cell LC_1 were 6.95 and 6.27 m s^{-1}, respectively while the short-lived cells were 5.21 and 3.67 m s^{-1} (4.82 and 3.65 m s^{-1} except the

cell SC_1), respectively. Though updraft and downdraft of long-lasting cell LC_1 were 1.5 times stronger than those of short-lived cells, the position of the updraft (or downdraft) and its interaction with adjacent cells could be more important than their intensity in facilitating the development and maintenance of convective cells over long periods.

In a future work, the temporal and vertical variation of the DSD parameters within the lifetimes of each precipitation cells will be discussed.

ACKNOWLEDGMENTS. This research was supported in part by a research fund of the Japanese Ministry of Land, Infrastructure, Transport and Tourism (MLIT). One of the authors (DIL) acknowledge support from the National Research Foundation of Korea (NRF) through a grant provided by the Korean Ministry of Education, Science & Technology (MEST) in 2011 (K20607010000).

REFERENCES

Browning, K. A., J. C. Fankhauser, J. P. Chalon and P. J. Ecolles, 1976: Structure of an evolving hailstorm, Part V: Synthesis and hail growth and hail suppression. *Mon. Wea. Rev.*, **104**, 603–611.

Byres, H. R., and R. R. Braham, 1949: *The Thunderstorm*. Washington, D.C., Government Printing Office, 287 pp.

Gao, j., M. Xue, A. Shapiro, and K. K. Droegemeier, 1999: A variational method for the analysis of three-dimensional wind fields from two Doppler radars. *Mon. Wea. Rev.*, **127**, 2128–2142.

Gorgucci, E., G. Scarchilli, and V. Chandrasekar, 1999: A procedure to calibrate multiparameter weather radar using properties of the rain medium. *IEEE Trans*. *Geosci. Remote Sens.*, **37**, 269–276.

Hobbs, P. V., and J. D. Locatelli, 1978: Rainbands, precipitation cores and generating cells in a cyclonic storm. *J. Atmos. Sci.*, **35**, 230–241.

Kato, Atsushi., and M. Maki, 2009: Localized heavy rainfall near Zoshigaya, Tokyo, Japan on 5 August 2008 observed by X-band polarimetirc radar: Preliminary analysis. *SOLA*, **5**, 089–092.

Kim, D.-S., M. Maki, and D.-I. Lee, 2008: Correction of X-band radar reflectivity and differential reflectivity for rain attenuation using differential phase. *J. Atmos. Res*., **90**, 1–9.

Kim, D.-S., M. Maki, and D.-I. Lee, 2010: Retrieval of three-dimensional raindrop size distribution using X-band polarimetric radar data. *J. Atmos*. *Oceanic Technol*., **27**, 1265–1285. LinY.-L., R. L. Deal, and M. S. Kulie, 1998: Mechanisms of cell regeneration, development, and propagation within a two-dimensional multicell storm. *J. Atmos. Sci*., **55**, 1867–1886.

Maki, M., S.-G. Park, and V. N. Bringi, 2005: Effect of natural variations in rain drop size distributions on rain rate estimators of 3 cm wavelength polarimetric radar. *J. Meteor. Soc. Japan*, **83**, 871–893.

Takeda, T. and K. Seko, 1986: Formation and maintenance of band-shaped convective radar echoes. J. Meteor. Soc. Japan, 64, 941–954.

Takeda, T., and H. Imai, 1976: On the behavior of long-lasting cellular Echoes. *J. Meteor. Soc. Japan*, 54, 399–406.

Warner, C., J. Simpson, G. van Helvoirt, D. W. Martin, D. Suchman, and G. L. Austin, 1980: Deep convection on day 261 of GATE. *Mon. Wea. Rev.*, **108**, 169–194.